Journal of Power Sources 325 (2016) 690–696

Contents lists available at ScienceDirect

Journal of Power Sources

journal homepage: www.elsevier.com/locate/jpowsour

Performance of single carbon granules as perspective for larger scale capacitive bioanodes

Casper Borsje [a, 1], Dandan Liu [a], Tom H.J.A. Sleutels [b], Cees J.N. Buisman [a, b], Annemiek ter Heijne [a, *]

[a] Sub-Department of Environmental Technology, Wageningen University, Bornse Weilanden 9, 6708 WG Wageningen, The Netherlands
[b] Wetsus, European Centre of Excellence for Sustainable Water Technology, Oostergoweg 9, 8911 MA Leeuwarden, The Netherlands

HIGHLIGHTS

- A single activated carbon granule produced 0.6 mA.
- Intermittent operation of activated carbon produced 2× more charge than graphite.
- Extrapolation to granular systems indicates untapped potential of capacitive MFCs.

GRAPHICAL ABSTRACT

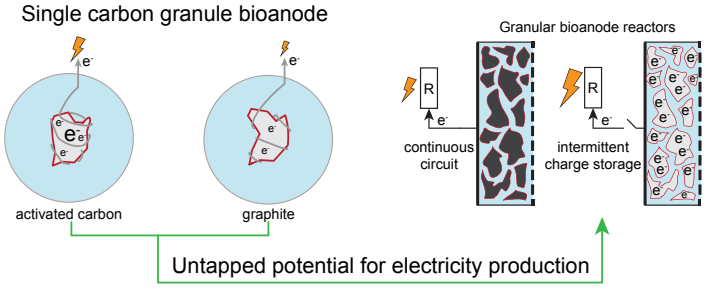

ARTICLE INFO

Article history:
Received 9 March 2016
Received in revised form
2 June 2016
Accepted 21 June 2016
Available online 27 June 2016

Keywords:
Microbial fuel cell
Capacitive bioanode
Granular bed
Activated carbon
Bioelectrochemical system

ABSTRACT

The use of high surface area electrodes, like carbon-based felt or granules, in Bioelectrochemical Systems is crucial for high volumetric current production. In case activated carbon granules are used, charge can also be stored in the form of an electric double layer in the pores, which has been shown to improve bioanode performance. So far, it is not known how much current can be generated by a single granule. In this study, we investigate the current production and charge storage behavior of a single carbon granule. Two types of activated carbon granules and one graphite granule are tested to find the untapped potential of granular bioanodes. A single activated carbon granule produces up to 0.6 mA, corresponding to 60 mA cm^{-3} granule volume at −300 mV vs. Ag/AgCl anode potential. Charge − discharge experiments show that capacitive granules produced 1.3–2.0 times more charge compared to a graphite granule with low surface area. When extrapolated to other granular systems, our study indicates that the current generated by granular bioanodes can be improved with several orders of magnitude, which could form the basis of an economically feasible Microbial Fuel Cell.

1. Introduction

The increasing global need for renewable resources is undeniable. In addition to sun and wind energy, soluble organic components in wastewater are a renewable resource. Electroactive microorganisms form the basis of bioelectrochemical systems (BESs), which are a promising technology for the conversion of

* Corresponding author. Postbox 17, 6700 AA, Wageningen, The Netherlands.
E-mail addresses: casper.borsje@wur.nl (C. Borsje), dandan.liu@wur.nl (D. Liu), tom.sleutels@wetsus.nl (T.H.J.A. Sleutels), cees.buisman@wur.nl (C.J.N. Buisman), annemiek.terheijne@wur.nl (A. ter Heijne).
[1] Present address: Wetsus, European Centre of Excellence for Sustainable Water Technology, Oostergoweg 9, 8911 MA, Leeuwarden, The Netherlands.

http://dx.doi.org/10.1016/j.jpowsour.2016.06.092

wastewater into other energy carriers. Electroactive microorganisms catalyze the oxidation of soluble organic components under anaerobic conditions. When they use the anode as electron acceptor, the microorganisms form a biofilm and the anode becomes a bioanode [1]. The application of a bioanode is found in two types of BESs. The first generates electrical power over an electrical load: a microbial fuel cell (MFC); the second utilizes power in addition to the oxidation of organics, to form products at the cathode, such as H_2, H_2O_2 and NaOH: a microbial electrolysis cell (MEC) [2]. Both systems simultaneously remove the organics from wastewater and produce a useful resource.

Conversion rates and energy recovery in bioanodes are still low when compared to biogas production through anaerobic digestion, even when taking into account significant losses for electricity production from biogas [3,4]. A strategy to enhance the conversion rate at the bioanode is the use of three-dimensional electrodes to provide more surface area for microbial growth per volume of reactor. These electrodes are often made of graphite felt [5–7], graphite granules or activated carbon granules [8–10]. An additional property of activated carbon granules is their high specific surface area (SSA), which is the surface area created by the porous structure of the carbon granules. An electric double layer (EDL) can form on this pore surface area in presence of an electrolyte [11]. In this EDL, electricity can be stored, acting as a capacitor, where high SSA generally relates to more charge storage: a property widely used in supercapacitor technologies [12]. Using activated carbon as a bioanode (Fig. 1) allows two processes to occur: (i) the electroactive biofilm releases electrons during the oxidation of organics (faradaic process), and (ii) these electrons are stored at the pore surface in the carbon, while cations are required to maintain the charge balance in the EDL (capacitive process) [13]. Following this concept, activated carbon granules have previously been integrated with the bioanode to form a capacitive bioanode, for in-situ charge storage [14], as well as in a fluidized bed reactor, where the granules are charged and discharged in separate locations [15].

While granular electrodes, both with high surface area (activated carbon granules) and with low surface area (graphite granules), have been applied as bioanodes, it is unknown how much current can actually be produced by one single granule. For this purpose, an MFC was developed to study one single granule. We investigated three types of granules: two types of activated carbon granules with high SSA, and one graphite granule with low SSA. We analyzed the current produced during continuous operation and the performance during intermittent charge and discharge cycles in terms of charge recovery.

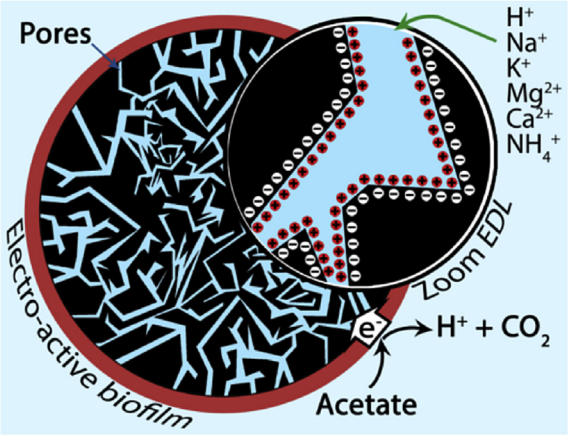

Fig. 1. The principle of capacitive granules with an electrochemically active biofilm. A faradaic reaction occurs when the biofilm oxidizes acetate and electrons are transferred to the activated carbon granule. This electron transfer, together with cation transport, leads to the formation of an electric double layer inside the pores so that charge is stored: a capacitive process.

2. Experimental

2.1. Setup of the single granule MFC

The single granule MFC was made of two Plexiglas plates, with a cylindrical chamber (13 mm diameter, 1 mL volume) drilled in each plate for an anode and cathode compartment (Fig. 2). The anode chamber contained the granule, held in place by a Pt wire (300 μm diameter, 17.9 g cm^{-3}), and a capillary for the reference electrode (3 M KCl Ag/AgCl, QM710X, ProSense Qis, Oosterhout, The Netherlands), see Fig. 2B. During assembly, multiple points of contact between wire and granule were ensured and, using a multimeter, the contact resistance was checked between wire and a point on the granule. We ensured the contact resistance was below 5 Ω. A cation exchange membrane (fumasep FKB, FuMa-Tech GmbH, St. Ingbert, Germany) separated the anode and cathode chambers. The cathode consisted of a piece of platinum foil connected to a stainless steel rod (Austenitic Corrosion Resisting Steel, Material No. 1.4539, ThyssenKrupp Materials International GmbH, Essen, Germany) as the current collector. An overview of the experimental set-up can be found in the supporting information (SI) chapter S1.

Three types of granules were used as anode: two activated carbon granules and one graphite granule. As a control, the Pt wire alone, without granule, was tested throughout the experiment. The activated carbon granules, with high SSA, were GAC830W, hereafter denoted as GAC, and PK1-3, hereafter denoted as PK, both from Cabot Norit Nederland B.V., Amersfoort, The Netherlands. The graphite granule, with low SSA, hereafter denoted as GG, was obtained from enViro-cell Umwelttechnik GmbH, Oberursel, Germany.

Though the current is a surface related process, it is singularly difficult to determine the surface area of a granule as used by the biofilm. As such, it was decided to use the volume as a normalization parameter, because of its usefulness for translating results to reactor performance. Through sieving, granules between 1 and 2 mm (stainless steel Analysensieb, Retsch, Haan, Germany) were obtained. The granules were further visually selected based on their comparable shape. As initial observations of mass and size indicated differences in density, the granule envelope volume was determined from the weight and envelope density. The envelop volume includes the solid carbon skeletal structure and the volume of the pores of the granule, and excludes the inter-granule volume of a granular bed [16]. The envelope volume, density (detailed information for its analysis in S2) of the granules and dry weight (dried for 24 h at 105 °C) of each granule is shown in Table 1.

2.2. Inoculum, media and operational strategy

The inoculum originated from a bioanode running on acetate. To obtain an active biofilm, the granules were first operated as a bioanode in a larger cell, completely filled with GAC granules, using a resistor of 1 kΩ and a 50 mM PBS buffer (pH 7) and a cathode open to air. After 2 weeks, one granule was transferred to the single granule MFC (GAC 17 days, PK and GG 21 days after inoculation).

The anode medium contained 10 mM $NaCH_3COO$, 0.2 g L^{-1} NH_4Cl, 10 mL L^{-1} Wolfe's Vitamin solution [17], 10 mL L^{-1} Wolfe's mineral solution [17] with 10.0 mg L^{-1} of Na_2SeO_3, $NiCl_2 \cdot 6H_2O$ and $Na_2WO_4 \cdot 2H_2O$ in 50 mM PBS buffer at pH 7 (5.43 g L^{-1} $Na_2HPO_4 \cdot 2H2O$, 2.65 g L^{-1} KH_2PO_4, 0.13 g L^{-1} KCl). The catholyte was a 100 mM K_3FeCN_6 solution in 50 mM PBS buffer at

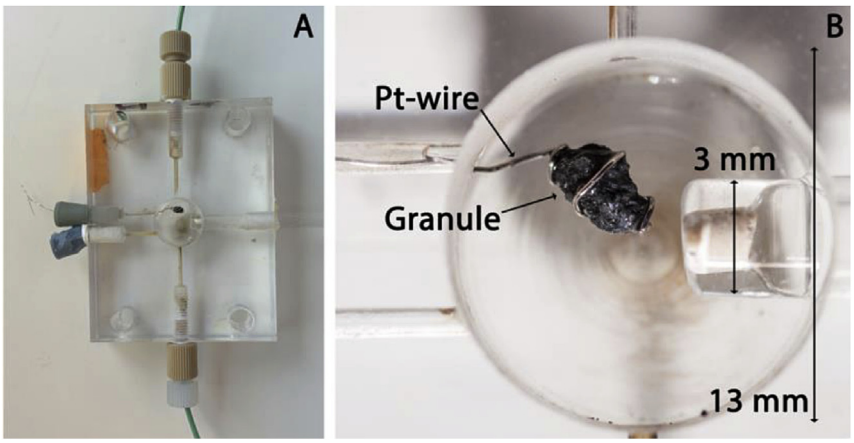

Fig. 2. A) The anode half-cell contains B) the anode compartment (volume of 1 mL and diameter of 13 mm) with capillary for reference electrode and graphite granule held by a Pt wire.

Table 1
Physical properties of the granules.

Granule	Mass (mg)	Density (g cm^{-3})	Volume (mm^3)
GAC	6.6 ± 0.1	1.06 ± 0.003	6.2 ± 0.1
PK	10.2 ± 0.1	1.03 ± 0.004	9.9 ± 0.1
GG	15.4 ± 0.1	2.13 ± 0.007	7.2 ± 0.1

pH 7. Temperature of the anolyte recirculation vessel was controlled at 35 °C in a water bath. Anaerobic conditions of the anolyte were created by continuous flushing with N_2. The electrolytes were replaced before the start of the electrochemical experiments (GAC 90 days, PK and GG 77 days after inoculation). The recirculation flow rate of anolyte and catholyte was between 0.5 (external resistance) and 2 (anode potential controlled) $mL.min^{-1}$.

During the growth phase in the singe granule MFC an external resistance of 1 MΩ was used, which was later decreased to 100 kΩ and 10 kΩ. This high resistance was chosen as not to draw too high currents from the small bioanode and thus damage the biofilm in its growth phase [18]. When the cell voltage stabilized at 10 kΩ, the electrochemical measurements were performed. The Pt wire control was connected via a 2 MΩ resistor to the cathode, during the entire experimental period. We used a higher resistance for the Pt wire than for the granule, because a lower current was expected from the Pt wire alone, because of its low surface area compared to the granules.

The anode potential and cell voltage over the external resistance were measured for each MFC throughout the experimental period and recorded every 60 s with LabVIEW and Fieldpoint modules (National Instruments Netherlands BV, Woerden, The Netherlands), except during electrochemical measurements.

2.3. Electrochemical experiments

All electrochemical measurements were performed using a potentiostat (Ivium n-Stat with IviumSoft v2.462 (Ivium Technologies BV, Eindhoven, The Netherlands), with the anode as working electrode. All potential values are reported versus Ag/AgCl reference (+205 mV vs. NHE). The measurements were recorded every 0.1 s.

2.3.1. Polarization curves

Polarization curves for granules with biofilm were recorded at anode potentials of −400, −300 and −200 mV for at least 600 s, up to 2 h for GAC and PK because of their higher capacitance, until the current was stable. The average current during the last 60 s of each potential was used for the polarization curve.

2.3.2. Constant potential charge and discharge

To determine the charge recovery of the high SSA granules compared to the low SSA granule, charge − discharge experiments were performed on the bioanodes. A single cycle consisted of 60 s Open Circuit (OC), followed by a discharge period of 180 s at a fixed anode potential. To ensure that each particle was equally discharged before the experiment at −300 mV, in line with previous work [9,10,15], the granules were discharged for 1 h before each charge − discharge experiment, from which the continuous current for each granule was taken as the average of the last 60 s. The stored charge can be determined by subtracting the total continuously produced charge from the total charge measured during discharge (total surface area of the current-time graph) [9]. The relative charge recovery η was calculated (equation (1)) over 40 sequential cycles. The relative charge recovery is used to compare the total accumulated volumetric charge (current integrated over total cycle time) of the intermittently operated active carbon bioanodes (PK and GAC) to the volumetric charge accumulated during continuous operation of the GG bioanode, which was considered as a non-capacitive granule because of its low SSA, in the same amount of time [10]:

$$\eta = Q_{\text{intermittent}} / Q_{\text{GG, continuous}} \quad (1)$$

2.4. Porosity characterization

To characterize the porous structure of the carbon granules, N_2 adsorption (77 K) was measured using Micromeritics Tristar 3000. SSA and pore size distribution (PSD) in the micropore (<2 nm) and mesopore (2–50 nm) range were analyzed using the Carbon-N_2 2D-NLDFT model [19] (Non Local Density Functional Theory). More details on the analysis can be found in S3.

3. Results and discussion

3.1. Current production of a single granule bioanode

After the growth phase, each granule reached a stable current. Fig. 3A shows the currents achieved during polarization curves. The

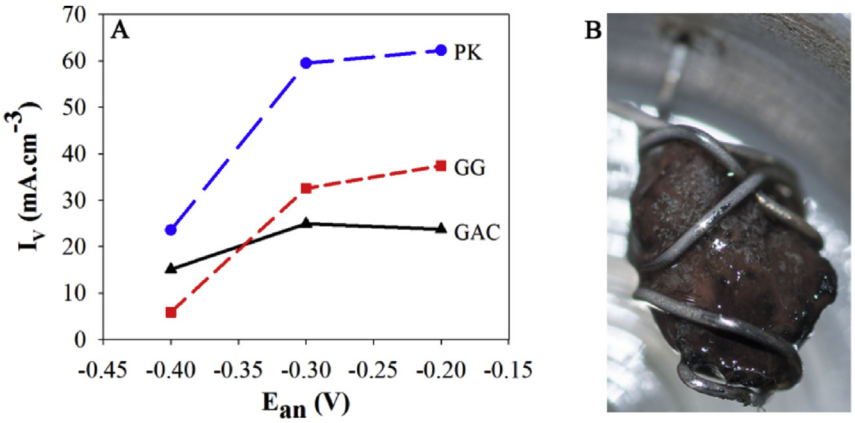

Fig. 3. A) The current densities, normalized to granule volume, achieved during polarization curves for the three granules. B) The PK granule as bioanode, photographed at the end of the experiment.

current density per volume of granule at an anode potential of −300 mV, which is the potential used in charge-discharge experiments, was 25 mA cm^{-3} (0.16 mA) for GAC, 60 mA cm^{-3} (0.59 mA) for PK and 33 mA cm^{-3} for GG (0.23 mA). The control experiment with only the Pt wire did not produce more than 0.154 mA cm^{-3} wire volume (0.32 μA at E_{an} = −313 mV) throughout the experiment, indicating that the current produced by the Pt wire as bioanode was negligible compared to the current produced by the bioanode granules. After opening the cell at the end of the experiments, a biofilm was observed during visual inspection (Fig. 3B).

3.2. Charge recovery of the capacitive bioanodes was higher than that of the graphite granule bioanode

The relative charge recovery (η) describes the efficiency of the charge transfer of a capacitive system, during charge and discharge cycles, as compared to a non-capacitive system in continuous operation. Previous work by Deeke et al. showed that charging and discharging of a capacitive anode resulted in an η of 1.0–1.3 compared to a graphite anode in a flat plate MFC [10], showing the enhanced current production for a capacitive MFC.

Fig. 4 shows the current (A) and anode potential (B) in time during a single cycle of charging (60 s) and discharging (180 s) of the three bioanode granules. During OC conditions, there is no current and electrons are stored in the granule. As a result, the anode potential decreases towards the equilibrium anode potential. During discharge, the anode potential is controlled at −300 mV, and because of the potential difference with the open circuit potential reached during charging, electrons are released from the granule. The current showed a peak, which is a combination of capacitive and faradaic current, after which the current decreased towards a stable value, which is the faradaic current continuously produced by the biofilm from conversion of acetate (without storage). The stored charge (Fig. 4A) was 9.7 times larger for the PK and 4.1 times larger for GAC granules compared to GG, which implies a higher capacitance compared to GG. The lower capacitance of GG resulted in a lower bioanode potential, while anode potential of GAC and PK decreased more slowly.

After 40 charge and discharge cycles, the accumulated charge over the total timespan was 318 C cm^{-3}, of which 59 C cm^{-3} stored (and discharged) charge, for GAC, 547 C cm^{-3}, of which 86 C cm^{-3} stored charge, for PK and 211 C cm^{-3}, of which 18 C cm^{-3} stored charge, for GG. In the same timespan 269 C cm^{-3} for GG was accumulated in continuous operation. This results in a η of 1.2 for GAC and 2.0 for PK, which indicates that both activated carbon granules in intermittent mode outperformed the GG granule in continuous mode. GG itself had an η of 0.8 – meaning that continuous operation results in better performance than intermittent operation. The results show the PK granule has the highest η, while the η of GAC is in the same range as found the capacitive anode by Deeke et al., which also composed of GAC type activated carbon [10].

3.3. Influence of porosity characteristics of the granules

N_2 adsorption was used to study the pore structure of the three

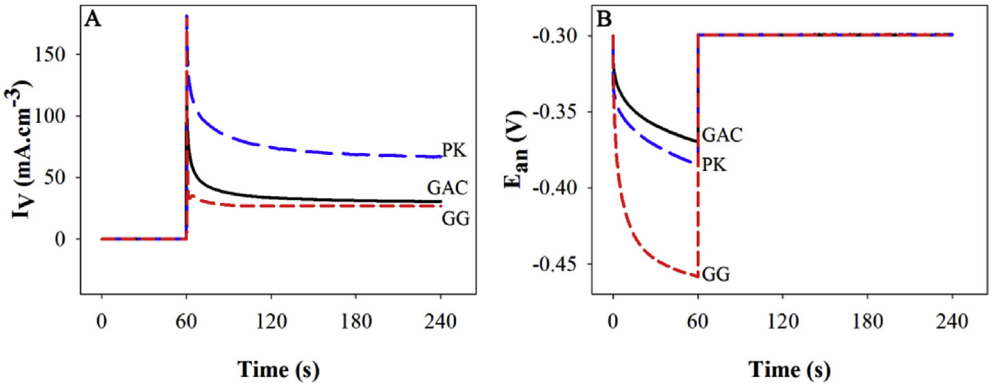

Fig. 4. One typical charge and discharge cycle, where charging occurred in the first 60 s, followed by a 180 s discharge period. A) Volumetric current density in time for the three granules. B) Anode potential in time during the same charging and discharging cycle.

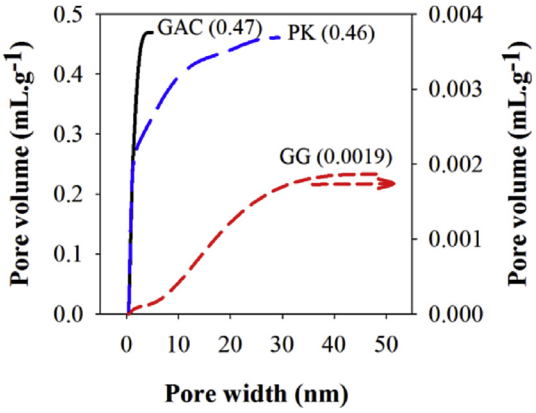

Fig. 5. Pore size distribution in the range of 0.3–50 nm: cumulative pore volume against the pore width for the three carbon granules. The total pore volume in the pore width range is shown.

granule types, in the pore width range 0.3–50 nm. The specific surface area (SSA) was 885 $m^2\ g^{-1}$ (940 $m^2\ cm^{-3}$) for GAC, 764 $m^2\ g^{-1}$ (790 $m^2\ cm^{-3}$) for PK and 0.438 $m^2\ g^{-1}$ (0.934 $m^2\ cm^{-3}$) for GG. In Fig. 5, the cumulative pore volume is shown as a function of the pore width. GAC and PK both showed about 250 times higher total pore volume than GG. The pore volume increased until 5 nm for GAC, until 29 nm for PK and for GG the pore volume increased up to the range limit of 50 nm. The microporosity (pore volume < 2 nm) was 80% of total pore volume for GAC, 60% for PK and 4% for GG and the mesoporosity (pore volume between 2 and 50 nm) was 20% of total pore volume for GAC, 40% for PK and 96% for GG. The combination of low SSA and high density indicates the pores of the GG granule are likely close to the external surface. It should be noted the SSA cannot be used for normalization of current, as the pores <50 nm are smaller than the bacteria themselves (e.g. *Geobacter sulferreducens* is about 1.7 μm long by 0.4 wide μm (based on 10 observations in the SEM image of an electrode surface from Bond and Lovely [20]).

From the polarization curve and Fig. 4, it can be seen that the continuous current densities of GAC and GG are similar and thus the biofilm activities are similar on the two granules. During the charge and discharge experiments, however, it is clear that more charge can be stored per cycle in GAC than in GG. As the biofilm activity for both granules is similar, it becomes clear that the physical granule properties, rather than possible capacitive properties of bioanode bacteria [21–25], are dominant for the charge storage. As the SSA is linked to the charge storage via surface available for EDL formation [11], the differences in NLDFT surface area, which is about 866 times higher for the GAC granule than for GG, can explain the larger storage capacity of GAC compared to GG. However, the 3.2 times higher charge storage cannot be explained by differences in SSA only. One possible explanation could be not all pore surface area is used, as Deeke et al. found increasing thickness of the capacitive layer of a capacitive bioanode decreased the charge stored [10].

The continuous current density of PK was 2.4 times higher than GAC, indicating that the biofilm activity was higher on PK granules. Similarly, PK had 2.3 times higher charge storage during the intermittent experiments compared to GAC. As the SSA of PK is lower than of GAC, the higher charge storage may be due to the higher biofilm activity. While the SSA of PK is lower than of GAC, it does have a higher mesoporosity. Although the higher mesoporosity has been shown to have a positive influence on the capacitance in supercapacitors and capacitive deionization [13,26–28], and could also affect charge storage by the capacitive bioanodes [10], other variables than the pore structure are likely to

Table 2
Table comparing single granule results to both intermittent and continuously operated systems found in literature.

Granules[a,b]	Cell type	Vanode (mL)	Vgranules (mL)	I_V (mA cm^{-3} reactor)	I_V (mA cm^{-3} granules)	Circuit[d]	Cathode	Source
Continuous operation								
GAC 830	Single chamber, packed bed	2,200[c]	1405	0.006	0.009	100 Ω resistor	n/a	[34]
GG[b1]	Two chamber, packed bed	350	182	0.063	0.121	10 Ω resistor	O_2 reduction	[4,31]
GG[b2]	Two chamber, packed bed, 6 in series	936	576	0.052	0.085	46 Ω resistor	$K_3Fe(CN)_6$	[4,33]
GG[b2]	Two chamber, packed bed	156	111	1.063	1.495	0 mV E_{an}	$K_3Fe(CN)_6$	[4,32]
GG[b3]	Two chamber tubular, packed bed	4900	2500	0.033	0.066	1 Ω resistor	Biological O_2 reduction	[4,30]
GAC	Two chamber, single granule	1	0.0062	0.155	24.958	−300 mV E_{an}	$K_3Fe(CN)_6$	This study
PK	Two chamber, single granule	1	0.0099	0.586	59.475	−300 mV E_{an}	$K_3Fe(CN)_6$	This study
GG	Two chamber, single granule	1	0.0072	0.231	31.934	−300 mV E_{an}	$K_3Fe(CN)_6$	This study
Intermittent operation								
GAC 1240	Fluidized bed, external discharge	2102	392	0.001	0.004	−300 mV E_{an}	$K_3Fe(CN)_6$	[15]
GAC 830	Fluidized bed, in situ discharge	3534	583	0.003	0.020	48 Ω resistor	O_2 reduction	[35]
GAC 3030	Fluidized bed, in situ discharge	7	1.14	0.260	1.603	1000 Ω resistor	O_2 reduction	[14]
GAC	Two chamber, single granule	1	0.0062	0.394	63.462[e]	−300 mV E_{an}	$K_3Fe(CN)_6$	This study
PK	Two chamber, single granule	1	0.0099	0.757	76.765[e]	−300 mV E_{an}	$K_3Fe(CN)_6$	This study
GG	Two chamber, single granule	1	0.0072	0.218	30.202[e]	−300 mV E_{an}	$K_3Fe(CN)_6$	This study

[a] GAC: Granular Activated Carbon in mesh size.
[b] GG: granular graphite with particle size distribution in mm diameter: [b1]2–6, [b2]1.5–5, [b3]average of 10.
[c] Single chamber system: reactor volume reported.
[d] E_{an}: anode potential versus Ag/AgCl reference electrode.
[e] Volumetric current density of the single granules during the intermittent operation were taken from the discharge only, as this is most consistent with operation in larger reactor systems where the current generated originates from the discharge of the capacitive granules.

be of influence as well. Properties such as surface roughness and surface chemistry could be different for each granule and might enhance the biofilm via surface availability (external surface per granule volume), protection from shear forces and biofilm attachment (e.g. hydrophobicity [29]). More investigation is required to identify the determining variables for the performance of granular systems.

3.4. Potential for higher performance in larger reactor systems

The volumetric current densities of the single granules have been determined for both the working volume (anode) and for the volume of the granule itself (via weight and envelope density), in order to compare the single granule results to bioelectrochemical granular anode reactors in previous studies. These reactors were either operated using continuous [30–34] or intermittent [14,15,35] harvesting the current from the granular anode. The results from the previous studies and the current densities of the single granules can be seen in Table 2.

The volumetric current densities of the single granules are several orders of magnitude higher than those reached by other systems. In continuous systems, current densities between 9 and 1500 A m^{-3} of granules, depending on reactor size and configuration, have been achieved [4,30–34]. The PK granule produced 43 to 7200 times higher current density than the currents reported in a granular bed reactor. Especially in larger reactors, the performance of these granules in continuous mode is low.

The comparison for granular bioanodes in intermittent operation shows a similar trend: currents between 4 and 1600 A m^{-3} of granules were reported [14,15,35], which are 48 to 21,000 times lower than the current density of the PK granule. Again, a similar trend is seen in that the smaller system performed much better than the large system.

There are several possible explanations for the low performance of both intermittent and continuous granular bioanodes compared to the single granule MFC, related to 1) contact, 2) flow and 3) biofilm damage. First, good contact between the granule and Pt wire was ensured and among the intermittently operated systems, increased collision force resulted in higher current density [14]. The second explanation is related to limited medium flow, where for the highest current density, homogeneity was ensured in the granular bed [32]. Third, the contact and sheer force between the granules and the current collector may damage the biofilm. From this comparison, it becomes apparent that there is much room for improvement in systems using granular bioanodes.

4. Conclusions

In this study, three single carbon granules were studied as bioanodes in a MFC. The highest volumetric current density was found using the PK activated carbon granule. In intermittent operation, where the charge storage in electrical double layer capacitance is used, the highest relative charge recovery of 2.0 and charge storage were found for the PK activated carbon as well, which was 4.7 times higher than the graphite granule. In comparison with other granular systems, it was shown that granular bioanodes can achieve much higher current densities than shown so far, especially if capacitive bioanodes are used. We demonstrate here a new test system in which single granules can be studied in detail, under continuous and intermittent operation strategies. This setup opens new opportunities to study bioanodes and to better understand the processes that determine the performance of granular electrodes. More insight in the performance of systems, that use capacitance by operating in intermittent mode, gives essential insights for further development of capacitive bioanodes in microbial fuel cells. If the untapped potential of a single granule can be realized on a larger scale, a big leap can be made towards practical application.

Acknowledgements

The research is supported by the Dutch Technology Foundation STW, which is part of the Netherlands Organization for Scientific Research (NWO), and which is partly funded by the Ministry of Economic Affairs (VENI grant no 13631).

The authors would like to thank Anneke Delsing and Miruna Florea, from Eindhoven University of Technology, for their help on the skeletal volume analysis of the carbon granules.

Glossary

BES	Bioelectrochemical System
MFC	Microbial Fuel Cell
MEC	Microbial Electrolysis Cell
SSA	Specific surface area
EDL	Electric double layer
η	relative charge recovery

Appendix A. Supplementary data

Supplementary data related to this article can be found at http://dx.doi.org/10.1016/j.jpowsour.2016.06.092.

References

[1] K. Rabaey, W. Verstraete, Trends Biotechnol. 23 (2005) 291–298.
[2] K. Rabaey, Bioelectrochemical Systems: from Extracellular Electron Transfer to Biotechnological Application, IWA Publishing, London, UK, 2010.
[3] T.H. Pham, K. Rabaey, P. Aelterman, P. Clauwaert, L. De Schamphelaire, N. Boon, W. Verstraete, Eng. Life Sci. 6 (2006) 285–292.
[4] J.B.A. Arends, W. Verstraete, Microb. Biotechnol. 5 (2012) 333–346.
[5] A. ter Heijne, H.V.M. Hamelers, C.J.N. Buisman, Environ. Sci. Technol. 41 (2007) 4130–4134.
[6] T.H.J.A. Sleutels, R. Lodder, H.V.M. Hamelers, C.J.N. Buisman, Int. J. Hydrogen Energy 34 (2009) 9655–9661.
[7] T.H.J.A. Sleutels, L. Darus, H.V.M. Hamelers, C.J.N. Buisman, Bioresour. Technol. 102 (2011) 11172–11176.
[8] C. Feng, Z. Lv, X. Yang, C. Wei, Phys. Chem. Chem. Phys. 16 (2014) 10464–10472.
[9] A. Deeke, T.H.J.A. Sleutels, H.V.M. Hamelers, C.J.N. Buisman, Environ. Sci. Technol. 46 (2012) 3554–3560.
[10] A. Deeke, T.H.J.A. Sleutels, A. ter Heijne, H.V.M. Hamelers, C.J.N. Buisman, J. Power Sources 243 (2013) 611–616.
[11] E. Frackowiak, F. Béguin, Carbon 39 (2001) 937–950.
[12] A. Schneuwly, R. Gallay, in: PCIM 2000, Rossens, Switzerland, 2000.
[13] S. Porada, R. Zhao, A. van der Wal, V. Presser, P.M. Biesheuvel, Prog. Mater. Sci. 58 (2013) 1388–1442.
[14] J. Liu, F. Zhang, W. He, X. Zhang, Y. Feng, B.E. Logan, J. Power Sources 261 (2014) 278–284.
[15] A. Deeke, T.H.J.A. Sleutels, T.F.W. Donkers, H.V.M. Hamelers, C.J.N. Buisman, A. ter Heijne, Environ. Sci. Technol. 49 (2015) 1929–1935.
[16] P.A. Webb, Micromeritics Instrum. Corp. 2 (2001) 01.
[17] E.A. Wolin, M.J. Wolin, R.S. Wolfe, J. Biol. Chem. 238 (1963) 2882–2886.
[18] Z. Ren, H. Yan, W. Wang, M.M. Mench, J.M. Regan, Environ. Sci. Technol. 45 (2011) 2435–2441.
[19] J. Jagiello, J.P. Olivier, Carbon 55 (2013) 70–80.
[20] D.R. Bond, D.R. Lovley, Appl. Environ. Microb. 69 (2003) 1548–1555.
[21] S. Freguia, K. Rabaey, Z. Yuan, J. Keller, Environ. Sci. Technol. 41 (2007) 2915–2921.
[22] G.D. Schrott, P.S. Bonanni, L. Robuschi, A. Esteve-Nuñez, J.P. Busalmen, Electrochim. Acta 56 (2011) 10791–10795.
[23] N. Uría, X. Muñoz Berbel, O. Sánchez, F.X. Muñoz, J. Mas, Environ. Sci. Technol. 45 (2011) 10250–10256.
[24] P.T. Ha, H. Moon, B.H. Kim, H.Y. Ng, I.S. Chang, Biosens. Bioelectron. 25 (2010) 1629–1634.
[25] Z. Lv, D. Xie, F. Li, Y. Hu, C. Wei, C. Feng, J. Power Sources 246 (2014) 642–649.
[26] L. Han, K.G. Karthikeyan, M.A. Anderson, K.B. Gregory, J. Colloid Interface Sci. 430 (2014) 93–99.
[27] S. Porada, L. Borchardt, M. Oschatz, M. Bryjak, J.S. Atchison, K.J. Keesman, S. Kaskel, P.M. Biesheuvel, V. Presser, Energy Environ. Sci. 6 (2013)

3700–3712.
[28] G. Gryglewicz, J. Machnikowski, E. Lorenc-Grabowska, G. Lota, E. Frackowiak, Electrochim. Acta 50 (2005) 1197–1206.
[29] C. Santoro, S. Babanova, K. Artyushkova, J.A. Cornejo, L. Ista, O. Bretschger, E. Marsili, P. Atanassov, A.J. Schuler, Bioelectrochemistry 106 (Part A) (2015) 141–149.
[30] F. Zhang, K.S. Jacobson, P. Torres, Z. He, Energy Environ. Sci. 3 (2010) 1347–1352.
[31] S. Freguia, K. Rabaey, Z. Yuan, J. Keller, Electrochim. Acta 53 (2007) 598–603.
[32] P. Aelterman, S. Freguia, J. Keller, W. Verstraete, K. Rabaey, Appl. Microbiol. Biotechnol. 78 (2008) 409–418.
[33] P. Aelterman, K. Rabaey, H.T. Pham, N. Boon, W. Verstraete, Environ. Sci. Technol. 40 (2006) 3388–3394.
[34] D. Jiang, B. Li, Biochem. Eng. J. 47 (2009) 31–37.
[35] J. Li, Z. Ge, Z. He, Bioresour. Technol. 167 (2014) 310–315.